THE UNIVERSITY of EDINBURGH

Edinburgh Research Explorer

Anthropogenic forcings and associated changes in fire risk in Western North America and Australia during 2015-2016

Citation for published version:
Tett, S, Falk, A, Rogers, M, Spuler, F, Turner, C, Wainwright, J, Dimdore-Miles, O, Knight, S, Freychet, N, Mineter, M & Lehmann, C 2018, 'Anthropogenic forcings and associated changes in fire risk in Western North America and Australia during 2015-2016' Bulletin of the American Meteorological Society. DOI: 10.1175/BAMS-D-17-0096.1

Digital Object Identifier (DOI):
10.1175/BAMS-D-17-0096.1

Link:
Link to publication record in Edinburgh Research Explorer

Document Version:
Publisher's PDF, also known as Version of record

Published In:
Bulletin of the American Meteorological Society

General rights
Copyright for the publications made accessible via the Edinburgh Research Explorer is retained by the author(s) and / or other copyright owners and it is a condition of accessing these publications that users recognise and abide by the legal requirements associated with these rights.

Take down policy
The University of Edinburgh has made every reasonable effort to ensure that Edinburgh Research Explorer content complies with UK legislation. If you believe that the public display of this file breaches copyright please contact openaccess@ed.ac.uk providing details, and we will remove access to the work immediately and investigate your claim.

Download date: 14. Jun. 2018

EXPLAINING EXTREME EVENTS OF 2016

From A Climate Perspective

Special Supplement to the
Bulletin of the American Meteorological Society
Vol. 99, No. 1, January 2018

EXPLAINING EXTREME EVENTS OF 2016 FROM A CLIMATE PERSPECTIVE

Editors

Stephanie C. Herring, Nikolaos Christidis, Andrew Hoell, James P. Kossin,
Carl J. Schreck III, and Peter A. Stott

Special Supplement to the

Bulletin of the American Meteorological Society

Vol. 99, No. 1, January 2018

American Meteorological Society

Corresponding Editor:

Stephanie C. Herring, PhD
NOAA National Centers for Environmental Information
325 Broadway, E/CC23, Rm 1B-131
Boulder, CO 80305-3328
E-mail: stephanie.herring@noaa.gov

Cover credit:

©The Ocean Agency / XL Catlin Seaview Survey / Chrisophe Bailhache—A panoramic image of coral bleaching at Lizard Island on the Great Barrier Reef, captured by The Ocean Agency / XL Catlin Seaview Survey / Christophe Bailhache in March 2016.

HOW TO CITE THIS DOCUMENT

Citing the complete report:

Herring, S. C., N. Christidis, A. Hoell, J. P. Kossin, C. J. Schreck III, and P. A. Stott, Eds., 2018: Explaining Extreme Events of 2016 from a Climate Perspective. *Bull. Amer. Meteor. Soc.*, **99** (1), S1–S157.

Citing a section (example):

Quan, X.W., M. Hoerling, L. Smith, J. Perlwitz, T. Zhang, A. Hoell, K. Wolter, and J. Eischeid, 2018: Extreme California Rains During Winter 2015/16: A Change in El Niño Teleconnection? [in "Explaining Extreme Events of 2016 from a Climate Perspective"]. *Bull. Amer. Meteor. Soc.*, **99** (1), S54–S59, doi:10.1175/BAMS-D-17-0118.1.

EDITORIAL AND PRODUCTION TEAM

Riddle, Deborah B., Lead Graphics Production, NOAA/NESDIS National Centers for Environmental Information, Asheville, NC

Love-Brotak, S. Elizabeth, Graphics Support, NOAA/NESDIS National Centers for Environmental Information, Asheville, NC

Veasey, Sara W., Visual Communications Team Lead, NOAA/NESDIS National Centers for Environmental Information, Asheville, NC

Fulford, Jennifer, Editorial Support, Telesolv Consulting LLC, NOAA/NESDIS National Centers for Environmental Information, Asheville, NC

Griffin, Jessicca, Graphics Support, Cooperative Institute for Climate and Satellites-NC, North Carolina State University, Asheville, NC

Misch, Deborah J., Graphics Support, Telesolv Consulting LLC, NOAA/NESDIS National Centers for Environmental Information, Asheville, NC

Osborne, Susan, Editorial Support, Telesolv Consulting LLC, NOAA/NESDIS National Centers for Environmental Information, Asheville, NC

Sprain, Mara, Editorial Support, LAC Group, NOAA/NESDIS National Centers for Environmental Information, Asheville, NC

Young, Teresa, Graphics Support, Telesolv Consulting LLC, NOAA/NESDIS National Centers for Environmental Information, Asheville, NC

TABLE OF CONTENTS

Abstract ii

1. Introduction to Explaining Extreme Events of 2016 from a Climate Perspective 1
2. Explaining Extreme Ocean Conditions Impacting Living Marine Resources 7
3. CMIP5 Model-based Assessment of Anthropogenic Influence on Record Global Warmth During 2016 11
4. The Extreme 2015/16 El Niño, in the Context of Historical Climate Variability and Change 16
5. Ecological Impacts of the 2015/16 El Niño in the Central Equatorial Pacific 21
6. Forcing of Multiyear Extreme Ocean Temperatures that Impacted California Current Living Marine Resources in 2016 27
7. CMIP5 Model-based Assessment of Anthropogenic Influence on Highly Anomalous Arctic Warmth During November–December 2016 34
8. The High Latitude Marine Heat Wave of 2016 and Its Impacts on Alaska 39
9. Anthropogenic and Natural Influences on Record 2016 Marine Heat waves 44
10. Extreme California Rains During Winter 2015/16: A Change in El Niño Teleconnection? 49
11. Was the January 2016 Mid-Atlantic Snowstorm "Jonas" Symptomatic of Climate Change? 54
12. Anthropogenic Forcings and Associated Changes in Fire Risk in Western North America and Australia During 2015/16 60
13. A Multimethod Attribution Analysis of the Prolonged Northeast Brazil Hydrometeorological Drought (2012–16) 65
14. Attribution of Wintertime Anticyclonic Stagnation Contributing to Air Pollution in Western Europe 70
15. Analysis of the Exceptionally Warm December 2015 in France Using Flow Analogues 76
16. Warm Winter, Wet Spring, and an Extreme Response in Ecosystem Functioning on the Iberian Peninsula 80
17. Anthropogenic Intensification of Southern African Flash Droughts as Exemplified by the 2015/16 Season 86
18. Anthropogenic Enhancement of Moderate-to-Strong El Niño Events Likely Contributed to Drought and Poor Harvests in Southern Africa During 2016 91
19. Climate Change Increased the Likelihood of the 2016 Heat Extremes in Asia 97
20. Extreme Rainfall (R20mm, RX5day) in Yangtze–Huai, China, in June–July 2016: The Role of ENSO and Anthropogenic Climate Change 102
21. Attribution of the July 2016 Extreme Precipitation Event Over China's Wuhang 107
22. Do Climate Change and El Niño Increase Likelihood of Yangtze River Extreme Rainfall? 113
23. Human Influence on the Record-breaking Cold Event in January of 2016 in Eastern China 118
24. Anthropogenic Influence on the Eastern China 2016 Super Cold Surge 123
25. The Hot and Dry April of 2016 in Thailand 128
26. The Effect of Increasing CO_2 on the Extreme September 2016 Rainfall Across Southeastern Australia 133
27. Natural Variability Not Climate Change Drove the Record Wet Winter in Southeast Australia 139
28. A Multifactor Risk Analysis of the Record 2016 Great Barrier Reef Bleaching 144
29. Severe Frosts in Western Australia in September 2016 150
30. Future Challenges in Event Attribution Methodologies 155

ABSTRACT—Stephanie C. Herring, Nikolaos Christidi, Andrew Hoell, James P. Kossin, Carl J. Schreck III, and Peter A. Stott

This sixth edition of explaining extreme events of the previous year (2016) from a climate perspective is the first of these reports to find that some extreme events were not possible in a preindustrial climate. The events were the 2016 record global heat, the heat across Asia, as well as a marine heat wave off the coast of Alaska. While these results are novel, they were not unexpected. Climate attribution scientists have been predicting that eventually the influence of human-caused climate change would become sufficiently strong as to push events beyond the bounds of natural variability alone. It was also predicted that we would first observe this phenomenon for heat events where the climate change influence is most pronounced. Additional retrospective analysis will reveal if, in fact, these are the first events of their kind or were simply some of the first to be discovered.

Last year, the editors emphasized the need for additional papers in the area of "impacts attribution" that investigate whether climate change's influence on the extreme event can subsequently be directly tied to a change in risk of the socio-economic or environmental impacts. Several papers in this year's report address this challenge, including Great Barrier Reef bleaching, living marine resources in the Pacific, and ecosystem productivity on the Iberian Peninsula. This is an increase over the number of impact attribution papers than in the past, and are hopefully a sign that research in this area will continue to expand in the future.

Other extreme weather event types in this year's edition include ocean heat waves, forest fires, snow storms, and frost, as well as heavy precipitation, drought, and extreme heat and cold events over land. There were a number of marine heat waves examined in this year's report, and all but one found a role for climate change in increasing the severity of the events. While human-caused climate change caused China's cold winter to be less likely, it did not influence U.S. storm Jonas which hit the mid-Atlantic in winter 2016.

As in past years, the papers submitted to this report are selected prior to knowing the final results of whether human-caused climate change influenced the event. The editors have and will continue to support the publication of papers that find no role for human-caused climate change because of their scientific value in both assessing attribution methodologies and in enhancing our understanding of how climate change is, and is not, impacting extremes. In this report, twenty-one of the twenty-seven papers in this edition identified climate change as a significant driver of an event, while six did not. Of the 131 papers now examined in this report over the last six years, approximately 65% have identified a role for climate change, while about 35% have not found an appreciable effect.

Looking ahead, we hope to continue to see improvements in how we assess the influence of human-induced climate change on extremes and the continued inclusion of stakeholder needs to inform the growth of the field and how the results can be applied in decision making. While it represents a considerable challenge to provide robust results that are clearly communicated for stakeholders to use as part of their decision-making processes, these annual reports are increasingly showing their potential to help meet such growing needs.

12. ANTHROPOGENIC FORCINGS AND ASSOCIATED CHANGES IN FIRE RISK IN WESTERN NORTH AMERICA AND AUSTRALIA DURING 2015/16

Simon F. B. Tett, Alexander Falk, Megan Rogers, Fiona Spuler, Calum Turner, Joshua Wainwright, Oscar Dimdore-Miles, Sam Knight, Nicolas Freychet, Michael J. Mineter, and Caroline E. R. Lehmann

Extreme vapor pressure deficits (VPD) have been associated with enhanced wildfire risk. Using one model, we found for 2015/16 that human influences quintupled the risk of extreme VPD for western North America and increased the risk for extratropical Australia.

Introduction. In 2016, about 3.6 million hectares of land burned in the United States and Canada (NIFC 2017; NFD 2017). In Canada, a wildfire southwest of Fort McMurray, Alberta, caused the largest wildfire evacuation in Alberta's history and destroyed 2400 homes in 2016 (McConnell 2016). Abatzoglou and Williams (2016; AP16 from hereon) showed that anthropogenic climate change has increased forest fire activity in the western United States. This raises the question if anthropogenic forcing are increasing the risk of devastating events outside this region such as the Canadian Fort McMurray fire.

During the Australian summer of 2015/16, the country experienced high numbers of bushfires: the southwest and southeast of the country were most affected with more than 100000 hectares of vegetation burned in Tasmania (ABC News 2016a). Over the course of this summer, 408 residential and 500 non-residential buildings were destroyed nationwide. This fire season was moderately destructive with insured losses of about AUD $350 million (ABC News 2016b).

AP16 found for the western United States a strong link between the spring–summer vapor pressure deficit (VPD) and the annual burned area. In this paper, we build on this work using monthly average VPD as a proxy for fire risk during the summer of 2016 for extratropical Australia (October–February) and western North America (May–August) though this link has not been directly established for either region. VPD is an absolute measure of the state of atmospheric moisture, specifically the difference between the saturation vapor pressure and the actual vapor pressure of the atmosphere (Seagar et al. 2015). Changes in VPD are associated with the drying of both live vegetation and litter fuels, and it is only when vegetation and litter fuels are sufficiently dry that fires can both ignite and spread (Bradstock 2010).

Methods. To estimate the effect of anthropogenic climate change on VPD in western North America and extratropical Australia, we compared three different ensembles of the HadAM3P atmosphere-only model (Massey et al. 2015), which has a resolution of 1.875° × 1.25°, with each other and the ERA-Interim (ERAI) reanalysis (Dee et al. 2011). The ensembles are:

- **Hist15–16**: Driven by observed sea surface temperatures (SST), sea ice coverage (SIC) as well as current concentrations of greenhouse gases and estimates of aerosol emissions (updated from Tett et al. 2013).
- **Nat15–16**: Driven by SST, SIC, greenhouse gases, and aerosol emissions as they are estimated to have been without human induced climate change with natural SST (Fig. ES12.1a) and SIC conditions described in the online supplement.
- **Historical:** Ensemble of 5 continuous simulations from December 1959 to November 2009 described by Tett et al. (2013).

Both Hist15–16 and Nat15–16 have 24 members, each using slightly different initial conditions, starting in December 2014 and ending in August 2016. We analyze the 12-month period September 2015 to

AFFILIATIONS: Tett, Rogers, Freychet, Mineter, and Lehmann—School of Geosciences, University of Edinburgh, Edinburgh, United Kingdom; Falk, Spuler, Turner, Wainwright, Dimdore-Miles, and Knight—School of Physics, University of Edinburgh, Edinburgh, United Kingdom.

DOI:10.1175/BAMS-D-17-0096.1

A supplement to this article is available online (10.1175/BAMS-D-17-0096.2)

August 2016. VPD is defined as (Seager et al. 2015; Wallace and Hobbs 2006):

$$VPD = e_S - e \;\&\; e_S = \frac{e}{RH}$$

and, neglecting moisture mass in the atmosphere, can be rewritten as:

$$VPD = \frac{M_{dry\,air}}{M_{H_2O}}\, q\, p^* \left(\frac{1}{RH} - 1\right) \qquad \text{Eq. (1)}$$

where $e(e_s)$ is the (saturated) vapor pressure, q the specific humidity, p^* the surface pressure, and RH the relative humidity near the surface.

We computed VPD in the HadAM3P simulations and ERAI reanalysis using Eq. (1) applied to gridded monthly mean data neglecting nonlinearity. For HadAM3P, q and RH were 1.5 meter values while for ERAI we interpolated q and RH from monthly mean pressure level data to the surface. We use as a reference period the 30 years 01 December 1979–30 November 2009 and VPD, $q_{sat}(q/RH)$, q, and p^* were converted to anomalies against this period from the Historical or ERAI values.

The western North America (WNA) region was defined as in Giorgi and Francisco (2000; GF00), while we defined an extratropical Australian region (extAUS) as the GF00 AUS region south of 23.5°S. Fire does not occur in all places in the regions, so we defined a fire-mask to keep locations in our analysis where fire occurs. This mask was constructed from the MODIS CMG dataset using *Aqua* satellite measurements (Giglio et al. 2009) for 2003–16. Each 0.5° × 0.5° grid box and climatological month, was defined as a fire grid box if the fraction of pixels with fire detected for 2003–16 was greater than 10^{-5} (Figs. ES12.1b–e show regions and fraction of fire pixels for January and July). The 10^{-5} is arbitrary and corresponds to roughly one detected fire pixel per month. Simulated (and reanalysis) VPD, q, RH, $q_{sat}(q/RH)$, and p^* anomalies and normals were bilinearly interpolated to this grid from the model/reanalysis grid, data only kept at fire grid boxes, and then area

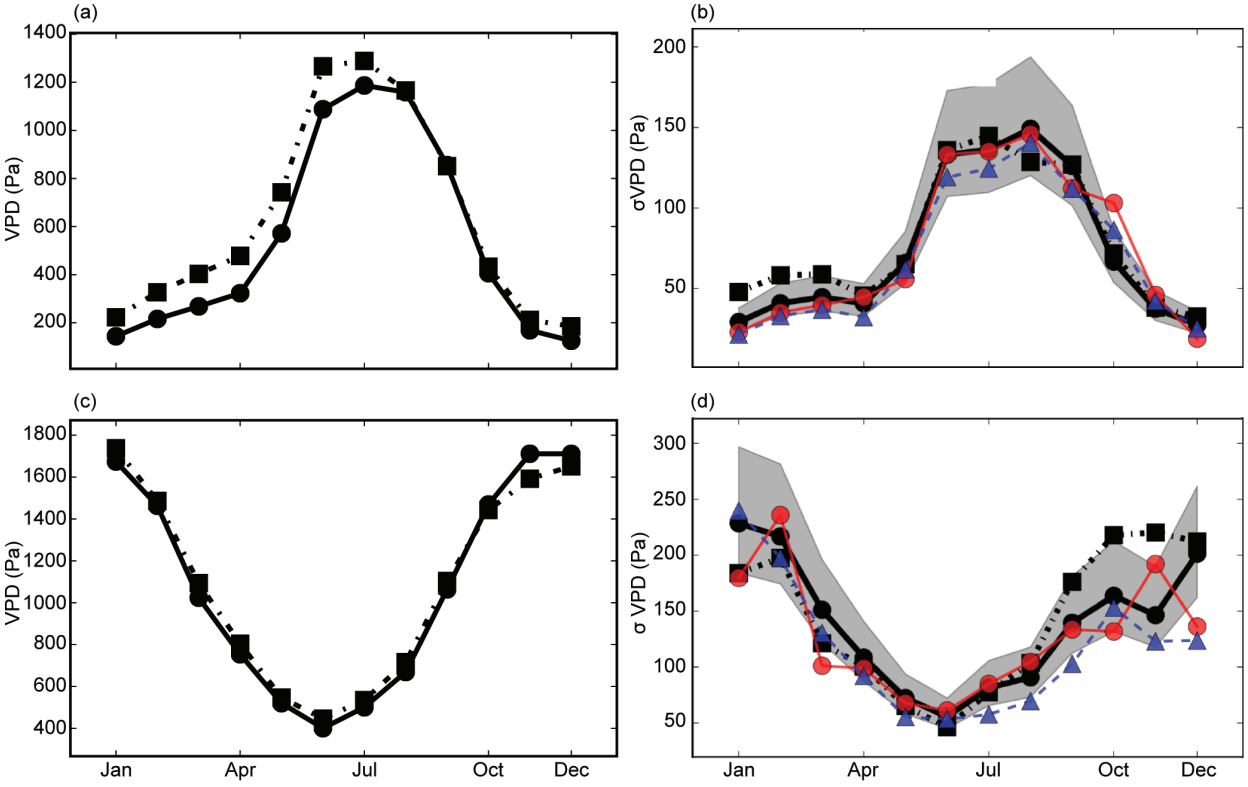

Fig. 12.1. VPD (Pa) comparison between ERAI (black dot-dashed, squares) and Historical (black lines, circles): (a),(c) 01 Dec 1979–Nov 2009 normals; (b),(d) std. dev. for WNA and extAUS, respectively. Gray shading indicates where reanalysis and Historical std. dev. are consistent (5%–95%). Std. dev for Sep 2105–Aug 2016 from Hist15–16 (red circles, lines) and Nat15–16 (blue triangles, dashed lines) are also shown in (b),(d). The x-axis on all plots shows climatological month (labels on bottom plots only).

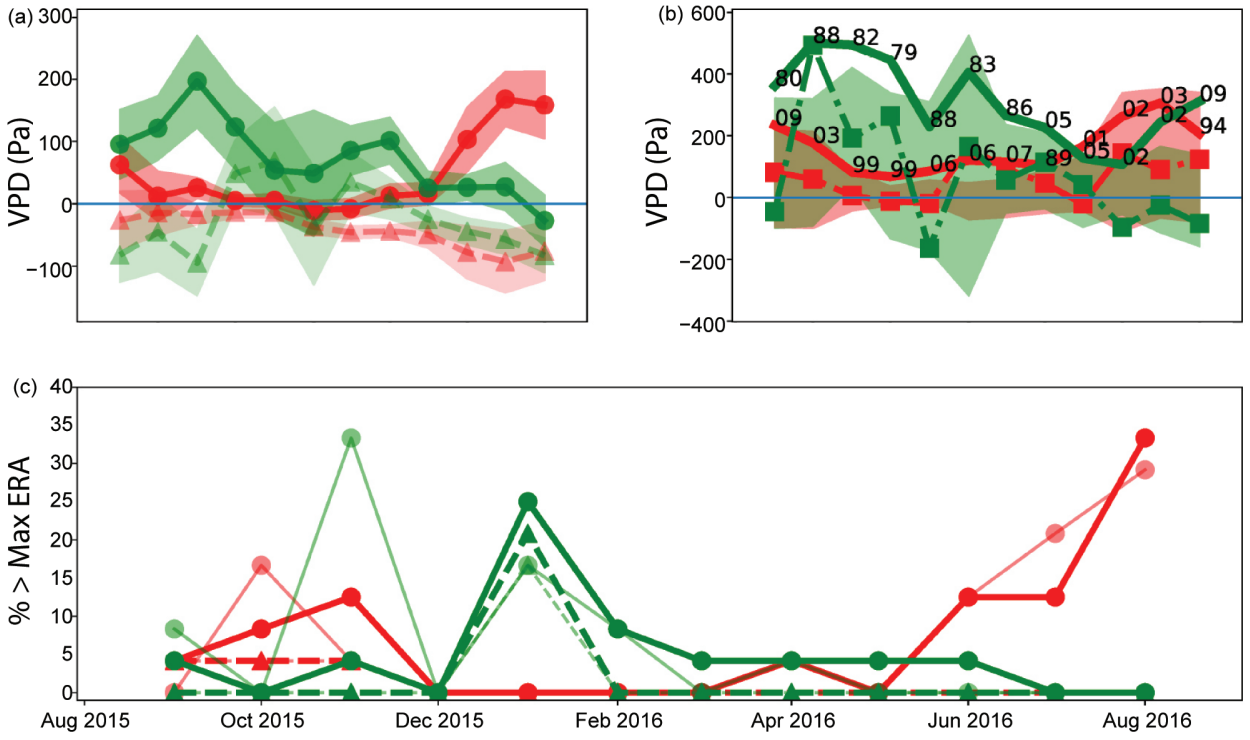

Fig. 12.2. (a) Ensemble-mean VPD anomalies (Pa) from Hist15–16 (circles) and Nat15–16 (triangles) for WNA (red) and extAUS (green). Shading shows ±2σ uncertainty. (b) Maximum VPD anomaly (Pa) for each climatological month [thick solid line and year (number) when max occurred] and anomaly for 15/16 (squares) from ERAI. Shading shows 5%–95% ranges from Hist15–16 ensemble with colors as (a). (c) Fraction (%) of Nat15–16 (dashed lines, triangles) and Hist15–16 (solid lines, circles) ensembles that exceeded 1979–2009 ERAI maximum VPD value for each month. Thin pale lines show same when anomalies scaled to correct for variance errors. All subplots use same common x-axis [values shown in (c)].

averaged over the two regions to produce time series. It is these time series that we subsequently analyze. Uncertainties on ensemble averages were computed by bootstrapping (Efron and Tibshirani 1994) over the ensemble members.

We define as a threshold for extreme events the ERAI maximum regional average VPD anomaly, for each calendar month, from the reference period corresponding to a one-in-30-year event. To compute the risk of exceeding this threshold we compute, for each month, the fraction of the Nat15–16 and Hist15–16 anomalies that exceed it. We test sensitivity to variance errors by scaling the Hist15–16 and Nat15–16 anomalies by the ratio of the monthly mean standard deviations from ERAI and Historical anomalies for the reference period.

Results. Model simulations are evaluated by comparing the Historical ensemble with ERAI. HadAM3P's VPD biases are small relative to the annual cycle though are negative for most of the year in WNA (Fig. 12.1a) with largest differences in June of –180 Pa. HadAM3P VPD variance appears consistent with that of ERAI (Fig. 12.1b) though the model has significantly smaller variance than ERAI for January–March, and there is no strong evidence of an increase in variability due to human forcings.

For extAUS Historical mean, VPD is, apart from November and December, consistent with that from ERAI (Fig. 12.1c). In November and December biases peak at about +120 Pa. Variability from reanalysis and HadAM3P is broadly consistent though reanalysis variability during austral summer is generally larger than simulated in HadAM3P. For most of the year, extAUS has larger variability in Hist15–16 and Historical than in Nat15–16 (Fig. 12.1d). Mean VPD values peak in WNA in June–August while in extAUS they are largest during October–February. It is these components of the annual cycle we subsequently focus on.

We now compare ensemble means from Hist15–16 with Nat15–16. For WNA, differences between the two ensembles are significant throughout most of the year with largest differences in July and August 2016 (Fig. 12.2a). For extAUS the Hist15–16 (Nat15–16)

ensemble has positive (negative) anomalies for most of the period suggesting that human influences have increased VPD. However, during December 2015 and January 2016 Nat15–16 shows positive anomalies.

We compare the Hist15–16 ensemble anomalies with ERAI (Fig. 12.2b). For both regions Hist15–16 is broadly consistent with ERAI though extAUS in October 2015, and WNA in February 2016 are exceptions to this (Fig. 12.2b). ERAI VPD values for September 2015 to August 2016, though generally larger than Nat15–16**,** are not very exceptional with almost all values being smaller than the maximum 1979–2009 VPD value. Maximum ERAI anomalies occur throughout the reference period with no obviously preferred year (or decade).

We now investigate the probability, for both ensembles, of crossing the 1979–2009 threshold. In extAUS, only in January 2016 do any of the Nat15–16 members cross the ERAI threshold (Fig. 12.2c). In WNA, the threshold is exceeded once in each of September through November 2015. For extAUS, there is an approximate doubling of the probability of exceeding the thresholds for October–February with a probability of about 7% (4%) for Hist15–16 (Nat15–16). May 2016, when the Fort McMurray fires started, has near-zero anomaly for WNA in both ensembles and reanalysis suggesting that this event was not strongly linked to continental scale VPD changes, and no ensemble members cross the 30-year threshold (Fig. 12.2c) during this month. However, during June 16–August 16, we find several extreme VPD values in the Hist15–16 ensemble, and no such events in the Nat15–16 ensemble (Fig. 12.2c). The average probability of crossing the threshold during this period is 19%. Making a relative risk estimate is difficult when the probability of events in the natural world are small. Being very conservative we assume, with 24 ensemble members, that the probability of crossing the threshold in Nat15–16 is 4% (1/24) giving a risk ratio of about 5, though larger values are possible.

We tested the sensitivity of these results to correcting for variance errors and found little sensitivity in WNA, but the risk for extAUS changed to 12% (3%) for Hist15–16 (Nat15–16) suggesting a risk ratio of about 4. Being conservative and taking the risk of 1:30 events for Nat15–16 as 4% then the risk of extreme VPD events, in extAUS, has increased by 2–3 times.

Our estimation of risk ratios is dependent on HadAM3P and the boundary conditions used. HadAM3P compares well with the ERAI VPD climatology (Fig. 12.1a) and the reanalysis values for September 2015–August 2016 are largely contained within the Hist15–16 ensemble (Fig. 12.2a). We decompose the changes in VPD into changes in saturated humidity, surface pressure, relative humidity, and residual effects (see online supplement and Fig. ES12.2). We find that changes in saturated humidity (likely dominated by changes in temperature) and relative humidity (likely model sensitive) are the dominant drivers of VPD in both regions. In WNA, changes in q_{sat} make the largest contribution with a small enhancement by reductions in *RH*. In contrast, for extAUS changes in *RH* offset changes in q_{sat} suggesting some model sensitivity in that region. Overall, we conclude that for WNA that human influences have very considerably increased the risk of extreme VPD values in June–August 2016, though not for the Fort McMurray fire period in May. For extratropical Australia, we find a weaker human influence with a doubling of the risk of extreme VPD. Assuming wildfire in extAUS and WNA, like in the western United States, is related to VPD then human influences have considerably increased the risk of one-in-30-year wildfire events.

ACKNOWLEDGMENTS. SFBT, MJM, and CERL supported by University of Edinburgh. NF supported by U.K.–China Research & Innovation Partnership Fund through the Met Office Climate Science for Service Partnership (CSSP) China as part of the Newton Fund. AF, MR, FS, CT, JW, O D-M, and SK carried out simulations and preliminary analysis as part of their coursework for "Introduction to three dimensional climate modelling" at University of Edinburgh. We thank the editor, two anonymous reviewers, and Stephanie Herring for comments that improved the paper, and Dathi Stone (LBL) for providing the Natural SST and SIC datasets. Data and software used in this paper are available from SFBT.

REFERENCES

ABC News, 2016a: *Major bushfires in Australia in 2015-2016 summer: Before and after*. ABC News [Australia] website, accessed 29 March 2017. [Available online at www.abc.net.au/news/2016-03-15/satellite-pictures-reveal-scale-of-summersbushfire-destruction/7232594.]

——, 2016b: *Catastrophic Summer events cost insurers more than $550 million,Insurance Council of Australia says*, ABC News [Australia] website, accessed 29 March 2017. [Available online at www.abc.net.au/news/2016-03-25/catastrophes-summer-costs-insurance-companies-more-than-550m/7276564.]

Abatzoglou, J. T., and A. P. Williams, 2016: Impact of anthropogenic climate change on wildfire across western US forests. *Proc. Natl. Acad. Sci. USA*, **113**, 11,770–11,775, doi:10.1073/pnas.1607171113.

Bradstock, R. A., 2010: A biogeographic model of fire regimes in Australia: Current and future implications. *Global Ecol. Biogeogr.*, **19**, 145–158, doi:10.1111/j.1466-8238.2009.00512.x.

Dee, D. P., and Coauthors, 2011: The ERA-Interim reanalysis: Configuration and performance of the data assimilation system. *Quart. J. Roy. Meteor. Soc.*, **137**, 553–597, doi:10.1002/qj.828.

Efron, B., and R. J. Tibshirani, 1994: *An Introduction to the Bootstrap*. CRC press, 456 pp.

Giglio, L., T. Loboda, D. P. Roy, B. Quayle, and C. O. Justice, 2009: An active-fire based burned area mapping algorithm for the MODIS sensor. *Remote Sens. Environ.*, 113, 408–420, doi:10.1016/j.rse.2008.10.006.

Giorgi, F., and R. Francisco, 2000: Uncertainties in regional climate change prediction: A regional analysis of ensemble simulations with the HADCM2 coupled AOGCM. *Climate Dyn.*, **16**, 169–192, doi:10.1007/PL00013733.

Massey, N., and Coauthors, 2015: weather@home—development and validation of a very large ensemble modelling system for probabilistic event attribution. *Quart. J. Roy. Meteor. Soc.*, **141**, 1528–1545, doi:10.1002/qj.2455.

McConnell, R., 2016: Fort McMurray is 'still alive,' fire chief says — but safety concerns linger. Canadian Broadcasting Corporation News, webstory. [Available at www.cbc.ca/news/canada/edmonton/fort-mcmurray-tour-notley-media-1.3572982, Date accessed 2017-03-29.]

NFD, 2017: National forest and forest management statistics. National Forestry Database [Canada], accessed 30 March 2017. [Available online at http://nfdp.ccfm.org/index_e.php.]

NIFC, [2017]: Total wildland fires and acres. National Interagency Fire Center [U.S.], accessed 29 March 2017. [Available at www.nifc.gov/fireInfo/fireInfo_stats_totalFires.html.]

Seager, R., A. Hooks, A. P. Williams, B. Cook, J. Nakamura, and N. Henderson, 2015: Climatology, variability, and trends in the U.S. vapor pressure deficit, an important fire-related meteorological quantity. *J. Appl. Meteor. Climatol.*, **54**, 1121–1141, doi:10.1175/JAMC-D-14-0321.1.

Tett, S. F. B., K. Deans, E. Mazza and J. Mollard, 2013: Are recent wet northwestern European summers a response to sea ice retreat? [in "Explaining Extreme Events of 2012 from a Climate Perspective"]. *Bull. Amer. Meteor. Soc.*, **94** (9), S32–S35.

Wallace, J., and P. Hobbs, 2006: *Atmospheric Science: An Introductory Survey*. 2nd ed. Academic Press, 483 pp.

Table 1.1. SUMMARY of RESULTS

ANTHROPOGENIC INFLUENCE ON EVENT			
	INCREASE	**DECREASE**	**NOT FOUND OR UNCERTAIN**
Heat	Ch. 3: Global Ch. 7: Arctic Ch. 15: France Ch. 19: Asia		
Cold		Ch. 23: China Ch. 24: China	
Heat & Dryness	Ch. 25: Thailand		
Marine Heat	Ch. 4: Central Equatorial Pacific Ch. 5: Central Equatorial Pacific Ch. 6: Pacific Northwest Ch. 8: North Pacific Ocean/Alaska Ch. 9: North Pacific Ocean/Alaska Ch. 9: Australia		Ch. 4: Eastern Equatorial Pacific
Heavy Precipitation	Ch. 20: South China Ch. 21: China (Wuhan) Ch. 22: China (Yangtze River)		Ch. 10: California (failed rains) Ch. 26: Australia Ch. 27: Australia
Frost	Ch. 29: Australia		
Winter Storm			Ch. 11: Mid-Atlantic U.S. Storm "Jonas"
Drought	Ch. 17: Southern Africa Ch. 18: Southern Africa		Ch. 13: Brazil
Atmospheric Circulation			Ch. 15: Europe
Stagnant Air			Ch. 14: Western Europe
Wildfires	Ch. 12: Canada & Australia (Vapor Pressure Deficits)		
Coral Bleaching	Ch. 5: Central Equatorial Pacific Ch. 28: Great Barrier Reef		
Ecosystem Function		Ch. 5: Central Equatorial Pacific (Chl-***a*** and primary production, sea bird abundance, reef fish abundance) Ch. 18: Southern Africa (Crop Yields)	
El Niño	Ch. 18: Southern Africa		Ch. 4: Equatorial Pacific (Amplitude)
TOTAL	18	3	9

	METHOD USED	Total Events
Heat	Ch. 3: CMIP5 multimodel coupled model assessment with piCont, historicalNat, and historical forcings Ch. 7: CMIP5 multimodel coupled model assessment with piCont, historicalNat, and historical forcings Ch. 15: Flow analogues conditional on circulation types Ch. 19: MIROC-AGCM atmosphere only model conditioned on SST patterns	
Cold	Ch. 23: HadGEM3-A (GA6) atmosphere only model conditioned on SST and SIC for 2016 and data fitted to GEV distribution Ch. 24: CMIP5 multimodel coupled model assessment	
Heat & Dryness	Ch. 25: HadGEM3-A N216 Atmosphere only model conditioned on SST patterns	
Marine Heat	Ch. 4: SST observations; SGS and GEV distributions; modeling with LIM and CGCMs (NCAR CESM-LE and GFDL FLOR-FA) Ch. 5: Observational extrapolation (OISST, HadISST, ERSST v4) Ch. 6: Observational extrapolation; CMIP5 multimodel coupled model assessment Ch. 8: Observational extrapolation; CMIP5 multimodel coupled model assessment Ch. 9: Observational extrapolation; CMIP5 multimodel coupled model assessment	
Heavy Precipitation	Ch. 10: CAM5 AMIP atmosphere only model conditioned on SST patterns and CESM1 CMIP single coupled model assessment Ch. 20: Observational extrapolation; CMIP5 and CESM multimodel coupled model assessment; auto-regressive models Ch. 21: Observational extrapolation; HadGEM3-A atmosphere only model conditioned on SST patterns; CMIP5 multimodel coupled model assessment with ROF Ch. 22: Observational extrapolation, CMIP5 multimodel coupled model assessment Ch. 26: BoM seasonal forecast attribution system and seasonal forecasts Ch. 27: CMIP5 multimodel coupled model assessment	
Frost	Ch. 29: *weather@home* multimodel atmosphere only models conditioned on SST patterns; BoM seasonal forecast attribution system	
Winter Storm	Ch. 11: ECHAM5 atmosphere only model conditioned on SST patterns	
Drought	Ch. 13: Observational extrapolation; weather@home multimodel atmosphere only models conditioned on SST patterns; HadGEM3-A and CMIP5 multimodel coupled model assessent; hydrological modeling Ch. 17: Observational extrapolation; CMIP5 multimodel coupled model assessment; VIC land surface hdyrological model, optimal fingerprint method Ch. 18: Observational extrapolation; *weather@home* multimodel atmosphere only models conditioned on SSTs, CMIP5 multimodel coupled model assessment	
Atmospheric Circulation	Ch. 15: Flow analogues distances analysis conditioned on circulation types	
Stagnant Air	Ch. 14: Observational extrapolation; Multimodel atmosphere only models conditioned on SST patterns including: HadGEM3-A model; EURO-CORDEX ensemble; EC-EARTH+RACMO ensemble	
Wildfires	Ch. 12: HadAM3 atmospere only model conditioned on SSTs and SIC for 2015/16	
Coral Bleaching	Ch. 5: Observations from NOAA Pacific Reef Assessment and Monitoring Program surveys Ch. 28: CMIP5 multimodel coupled model assessment; Observations of climatic and environmental conditions (NASA GES DISC, HadCRUT4, NOAA OISSTV2)	
Ecosystem Function	Ch. 5: Observations of reef fish from NOAA Pacific Reef Assessment and Monitoring Program surveys; visual observations of seabirds from USFWS surveys. Ch. 18: Empirical yield/rainfall model	
El Niño	Ch. 4: SST observations; SGS and GEV distributions; modeling with LIM and CGCMs (NCAR CESM-LE and GFDL FLOR-FA) Ch. 18: Observational extrapolation; *weather@home* multimodel atmosphere only models conditioned on SSTs, CMIP5 multimodel coupled model assessment	
		30